Monostatic coaxial 1.5 m laser Doppler velocimeter using a scanning Fabry-Perot interferometer

Rodrigo, Peter John; Pedersen, Christian

Published in:
Optics Express

Link to article, DOI:
10.1364/OE.21.021105

Publication date:
2013

Document Version
Publisher's PDF, also known as Version of record

Monostatic coaxial 1.5 μm laser Doppler velocimeter using a scanning Fabry-Perot interferometer

Peter John Rodrigo* **and Christian Pedersen**

DTU Fotonik, Department of Photonics Engineering, Technical University of Denmark, Frederiksborgvej 399, 4000 Roskilde, Denmark

pejr@fotonik.dtu.dk

Abstract: We present a laser Doppler velocimeter (LDV) in monostatic coaxial arrangement consisting of off-the-shelf telecom-grade components: a single frequency laser (wavelength λ = 1.5 μm) and a high-finesse scanning Fabry-Perot interferometer (sFPI). In contrast to previous 1.5 μm LDV systems based on heterodyne detection, our sFPI-LDV has the advantages of having large remote sensing range not limited by laser coherence, high velocity dynamic range not limited by detector bandwidth and inherent sign discrimination of Doppler shift. The more optically efficient coaxial arrangement where transmitter and receiver optics share a common axis reduces the number of components and greatly simplifies the optical alignment. However, the sensitivity to unwanted backreflections is increased. To circumvent this problem, we employ a custom optical circulator design which compared to commercial fiber-optic circulator achieves ~40 dB reduction in strength of unwanted reflections (i.e. leakage) while maintaining high optical efficiency. Experiments with a solid target demonstrate the performance of the sFPI-LDV system with high sensitivity down to pW level at present update rates up to 10 Hz.

OCIS codes: (280.0280) Remote sensing and sensors; (280.3340) Laser Doppler velocimetry; (120.2230) Fabry-Perot.

References and links

1. J. W. Czarske, "Laser Doppler velocimetry using powerful solid-state light sources," Meas. Sci. Technol. **17**(7), R71–R91 (2006).
2. T. O. H. Charrett, S. W. James, and R. P. Tatam, "Optical fibre laser velocimetry: a review," Meas. Sci. Technol. **23**(3), 032001 (2012).
3. N. A. Halliwell, "Laser vibrometry," in *Optical Methods in Engineering Metrology*, D. C. Williams, ed. (Chapman and Hall, 1993) pp. 179–211.
4. M. S. Stieglmeier and C. Tropea, "Mobile fiber-optic laser Doppler anemometer," Appl. Opt. **31**(21), 4096–4105 (1992).
5. W. T. Buttler and S. K. Lamoreaux, "Optical heterodyne accelerometry: passively stabilized, fully balanced velocity interferometer system for any reflector," Appl. Opt. **49**(23), 4427–4433 (2010).
6. C. F. McMillan, D. R. Goosman, N. L. Parker, L. L. Steinmetz, H. H. Chau, T. Huen, R. K. Whipkey, and S. J. Perry, "Velocimetry of fast surfaces using Fabry-Perot interferometry," Rev. Sci. Instrum. **59**(1), 1–21 (1988).
7. H. W. Mocker and P. E. Bjork, "High accuracy laser Doppler velocimeter using stable long-wavelength semiconductor lasers," Appl. Opt. **28**(22), 4914–4919 (1989).
8. M. Harris, G. Constant, and C. Ward, "Continuous-Wave Bistatic Laser Doppler Wind Sensor," Appl. Opt. **40**(9), 1501–1506 (2001).
9. D. A. Jackson and D. M. Paul, "Measurement of hypersonic velocities and turbulences by direct spectral analysis of Doppler shifted laser light," Phys. Lett. A **32**(2), 77–78 (1970).
10. M. Hercher, "The spherical mirror fabry-perot interferometer," Appl. Opt. **7**(5), 951–966 (1968).
11. M. Harris, G. N. Pearson, J. M. Vaughan, D. Letalick, and C. J. Karlsson, "The role of laser coherence length in continuous-wave coherent laser radar," J. Mod. Opt. **45**(8), 1567–1581 (1998).
12. P. J. Rodrigo and C. Pedersen, "Field performance of an all-semiconductor laser coherent Doppler lidar," Opt. Lett. **37**(12), 2277–2279 (2012).
13. J. Cooper and J. R. Greig, "Rapid scanning of spectral line profiles using an oscillating Fabry-Pérot interferometer," J. Sci. Instrum. **40**(9), 433–437 (1963).

#193983 - $15.00 USD Received 16 Jul 2013; revised 14 Aug 2013; accepted 22 Aug 2013; published 3 Sep 2013

1. Introduction

Laser Doppler velocimetry (LDV) has become a ubiquitous tool for the noncontact measurement of velocity of a moving target [1, 2]. The measurement principle relies on the detection of radial Doppler shift imparted on light scattered off the target. In LDV, one or more incident laser beams are used to probe various types of target ranging from fluid-borne microscopic particles to opaque reflecting surfaces. This enabled LDV to be applied to a number of applications in fluid mechanics [1], aerodynamics [3], vibrometry [4], and shock physics [5, 6].

LDV systems can be broadly classified into two main categories [2]: (1) the heterodyne detection LDV and (2) the direct detection LDV. In heterodyne detection LDV, the reference beam (local oscillator) is coherently mixed with the scattered signal beam onto a photodetector. Measuring the frequency of the resulting photocurrent beat signal gives the Doppler shift, f_D. The measured shift then determines the magnitude of the target's velocity component along the line-of-sight (LOS) of the incident beam according to a simple relation given by

$$f_D = \frac{1}{\pi}\vec{k}\cdot\vec{v} = \frac{2}{\lambda}v_{LOS}, \tag{1}$$

where $\vec{v}$ is the velocity vector, v_{LOS} is the line-of-sight speed, and $\vec{k}$ and λ are the k-vector and the wavelength of the incident beam, respectively. In direct detection LDV, the signal beam scattered off the target is sent "directly" to a frequency-to-intensity converter (e.g. optical filter) or an optical spectrum analyzer (OSA) with sufficient resolution. With an OSA, Doppler shift (and hence v_{LOS} using Eq. (1)) is obtained by simply taking the difference in center frequencies of the spectral line profiles of the scattered and the reference beams.

In many applications, the primary considerations in LDV designs include eye safety, long sensing range capability and large measured speed limit. Eye safety requirement is much more relaxed when using laser emitters that operate in the infrared wavelength range of 1500-1600 nm. Operating in this spectral band allows for additional benefits due to both high availability and high quality of components from the well-established telecommunications industry. However, only a few LDV systems operating in this eye-safe spectral region have been reported in the literature. Mocker and Bjork [7] previously demonstrated an LDV system that employed an external cavity InGaAsP diode laser operating at 1.54 μm wavelength and 40 kHz linewidth. Another LDV embodiment developed by Buttler and Lamoreaux for remotely probing explosively driven surfaces [5] used a fiber-laser operating at 1.5 μm and <10 kHz linewidth. Both of these LDVs are based on the heterodyne detection which requires very narrow linewidth (i.e. long coherence length) sources to achieve long range capability and very high bandwidth photodetectors to measure large velocities. The 1.5 μm LDV proposed in this work is based on direct detection which, unlike heterodyne detection, relaxes the requirement on laser linewidth and detector bandwidth, and also circumvents local oscillator shot noise. Similar to heterodyne detection, our proposed direct detection LDV is insensitive to laser frequency drift since the Doppler shift of the signal is measured relative to the center frequency of a reference beam tapped from the laser transmitter itself.

In this work, we demonstrate what to our knowledge is the first 1.5 μm direct detection LDV in which a scanning Fabry-Perot interferometer (sFPI) is utilized as a high-resolution OSA. In addition, we employ a monostatic coaxial architecture to achieve high optical receiver efficiency and easy alignment, which are the main drawbacks in bistatic or biaxial designs [8]. The use of sFPI in Doppler velocimetry was first demonstrated by Jackson and Paul in 1970 [9]. However, their LDV used a biaxial arrangement and an Ar^+ laser source – limiting the system in terms of optical receiver efficiency, eye safety and compactness. Here we demonstrate a more compact and more optically efficient monostatic coaxial LDV using a fiber-laser (λ = 1575 nm) and a high-finesse sFPI with an InGaAs transimpedance amplified photodetector measuring the output beam power through the sFPI. The use of a monostatic

#193983 - $15.00 USD Received 16 Jul 2013; revised 14 Aug 2013; accepted 22 Aug 2013; published 3 Sep 2013

coaxial design over a biaxial arrangement reduces the number of components and system footprint but suffers from increased sensitivity to unwanted reflections originating from optical surfaces. To address this challenge, we have employed a custom circulator which dramatically reduced the power level of stray reflections by 4 order orders of magnitude compared to the leakage found in standard fiber-optic circulators.

2. Measurement principle of sFPI-LDV

A scanning Fabry-Perot interferometer is commonly used as a high resolution OSA of an input radiation. The sFPI employed in this work uses two identical spherical mirrors whose radius of curvature defines the confocal mirror separation d. For spectral analysis, one mirror is scanned to change the separation from $d \rightarrow d + \delta$. A small change $\delta = \lambda/4$ ($\delta << d$) corresponds to one free spectral range [10],

$$\mathrm{FSR} = \frac{c}{4nd}, \tag{2}$$

which is a span of frequency within which unambiguous spectral assignment by the sFPI is possible (c is the vacuum light speed and n is the refractive index of air between the mirrors). For narrowband monochromatic light, scanning the mirror by a piezoelectric actuator driven with a linear ramp voltage, V_{ramp}, results in output detector voltage, V_{det}, which describes the temporal variation in interferometer transmission during scan as shown in Fig. 1(a). Assuming displacement δ is linear with drive voltage V_{ramp}, the horizontal axis also denotes frequency axis with two successive resonance peaks (i.e. transmission maxima) exactly at one full FSR separation. For a true monochromatic spectral line, the full-width-at-half-maximum (FWHM) of a resonance peak gives the width of the instrument profile

$$\Delta \mathrm{f}_{\mathrm{FPI}} = \frac{c}{4nd}\frac{(1-R)}{\pi\sqrt{R}} = \frac{\mathrm{FSR}}{F}, \tag{3}$$

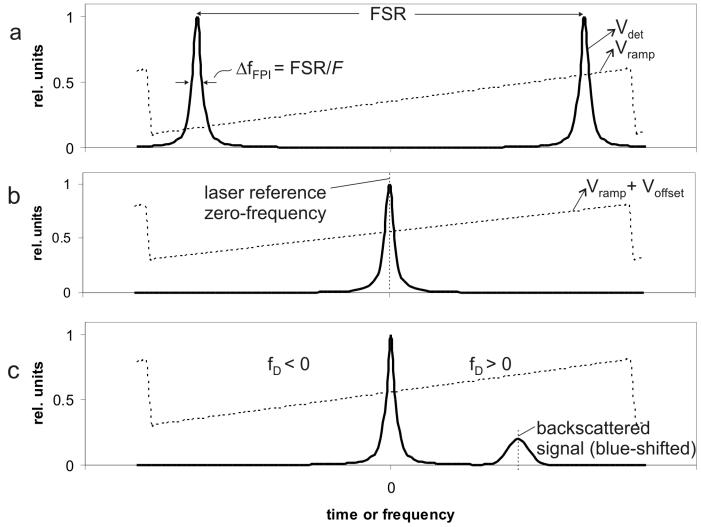

Fig. 1. (a) Typical relationship between output detector voltage V_{det} and ramp voltage V_{ramp} applied to the piezo-driven mirror of the sFPI. (b) Addition of an appropriate constant voltage V_{offset} to V_{ramp} allows for positioning of a laser reference resonance peak at the center of the scan. (c) Simultaneous measurement of center frequencies of the laser reference and target backscattered signal results in determination of both magnitude and sign of the Doppler shift f_D.

#193983 - $15.00 USD Received 16 Jul 2013; revised 14 Aug 2013; accepted 22 Aug 2013; published 3 Sep 2013

where $F = \pi\sqrt{R}/(1 - R)$ is the so-called finesse. A DC offset, V_{offset}, may be added to the ramp voltage to center the position of a resonance peak as a location of zero-frequency as depicted in Fig. 1(b). If the sFPI analyzes both reference laser and backscattered signal beams, and the signal beam is blue-shifted, a secondary peak corresponding to the signal appears to one side of the reference peak as shown in Fig. 1(c). It will appear shifted to the opposite side for a red-shifted signal beam. Thus, the possible dynamic range for Doppler shift measurement with sign-discrimination is from –½FSR to + ½FSR (or 0 to FSR for one where sign information is not required). With a few centimeters of mirror separation *d*, FSR in the order of GHz is achieved – resulting in the ability to measure supersonic speeds [9]. The FSR of the sFPI used in this work is 1 GHz, which for λ = 1.5 μm corresponds to a maximum v_{LOS} dynamic range of –375 m/s to + 375 m/s (or 0 to 775 m/s).

For moderate v_{LOS} ranging from, say, –30 m/s to + 30 m/s (Doppler shift from –40 MHz to + 40 MHz for λ = 1.5 μm), instead of using longer cavity design, it is more practical to utilize short mirror spacing due to alignment and stability considerations (i.e. thermal expansion, vibrations). For a fixed *F*, smaller *d* has the penalty of resulting in broader resonance peak. Nonetheless, sufficient Δf_{FPI} in the order of 1 MHz is attainable even with 1 GHz FSR (*d* = 75 mm) due to the availability of high quality mirrors that allow for relatively large finesse values (*F* ~1000). Although applicable to high velocity measurements up to few hundreds of meters per second, a 1 GHz FSR interferometer can operate at reduced scan range (i.e. frequency range < FSR) more appropriate for moderate speeds.

The sFPI-LDV has several advantages over the heterodyne detection LDV. Because the required reference signal is much weaker (typically ~10 pW versus ~1 mW local oscillator in heterodyne detection), the sFPI-LDV is not strongly affected by local oscillator shot noise and has a more relaxed phase noise and/or coherence length requirements of the laser source unlike heterodyne detection [11]. Laser linewidth affects the speed resolution but not the maximum sensing range of our direct detection LDV whereas in heterodyne detection it is normally limited by the coherence length. As mentioned above, the sFPI-LDV can easily measure Doppler-shifted signals in the 1 GHz range (corresponding to 750 m/s at 1500 nm wavelength) thus addressing applications requiring high velocity measurements for which a heterodyne LDV would require higher bandwidth detectors and high speed A/D converters [5, 7] in order to satisfy the Nyquist sampling criterion. The sFPI-LDV has an inherent ability to measure the sign of Doppler shift without the need for additional components like acousto-optic modulator or frequency shifter. Furthermore, the sFPI-LDV requires a much simpler data acquisition and data processing (while heterodyne detection involves FFT processing typically implemented on an FPGA board [12]), thus reducing cost and development complexity.

There are, however, technical challenges associated with the sFPI-LDV not present in its heterodyne counterpart. For weak backscattered signal, sFPI-LDV requires the use of a photodetector sensitive to low light levels. These commercially available detectors typical have low saturation, e.g. ~100 pW of incident optical power. This means the sFPI-LDV is highly sensitive to background or stray light usually reflected from interfaces in the system's optical train. In addition, the sFPI-LDV measurement principle is more sensitive to temperature variation. In the discussion of our experimental results below, we consider how the above problems can be mitigated.

3. Experimental setup

Our proposed LDV design consists of three main parts: (1) laser, (2) optical transceiver and (3) scanning Fabry-Perot interferometer (sFPI). We tested two embodiments which essentially differ in their optical transceiver parts. Embodiment #1 uses a standard single-mode fiber-optic circulator (6015-3-APC, Thorlabs Inc.) as shown in Fig. 2(a) while embodiment #2 uses a custom-made circulator as shown in Fig. 2(b) comprising a thin-film polarization (TFP) splitter, a zero-order $\lambda/4$ plate, and a set of aspheric lenses. Furthermore, the incident beam probing the solid target (rotating disk) in Fig. 2(a) is generally elliptically

#193983 - $15.00 USD Received 16 Jul 2013; revised 14 Aug 2013; accepted 22 Aug 2013; published 3 Sep 2013

polarized while in Fig. 2(b) it is circularly polarized. This difference in incident polarization can be ignored here since the solid target we used cause negligible depolarization effects. Both employ a commercial off-the-shelf scanning Fabry-Perot interferometer (FPI 100, Toptica Photonics AG). Unlike in a previous sFPI-LDV demonstration with bistatic or biaxial design [8], our setups use monostatic coaxial arrangement that provides for easy alignment and better receiver efficiency. Instead of photon counter, we use an InGaAs photodetector with built-in transimpedance amplifier (LCA-S femtowatt photoreceiver, FEMTO GmbH). This detector has a specified noise equivalent power or NEP = 2.3 fW/Hz$^{1/2}$ and a bandwidth B = 200 Hz.

The LDV performance is experimentally verified by measuring the v_{LOS} of a probed point on a tilted rotating disk positioned in the vicinity of the transmit beam waist (Fig. 2). To operate at eye-safe wavelength we use a 1575 nm fiber-laser (Koheras AdjustiK, NKT Photonics A/S).

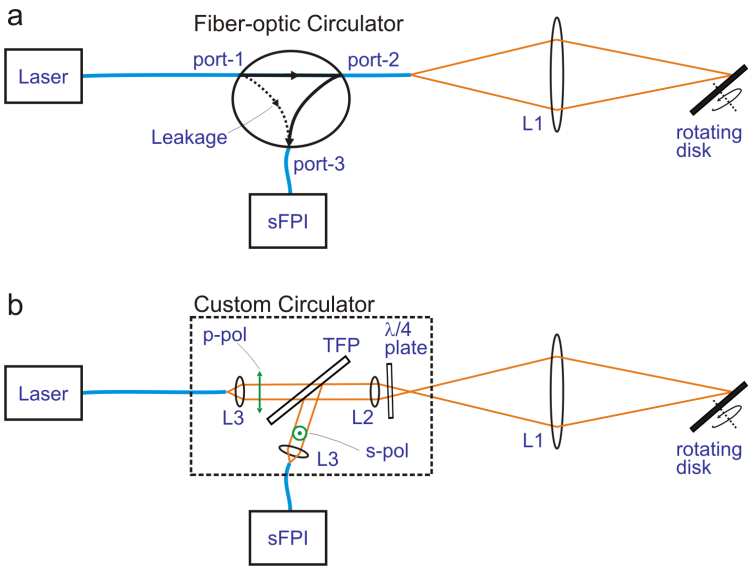

Fig. 2. Experimental setups used to test the performance of the proposed monostatic coaxial sFPI-LDV: (a) using standard fiber-optic circulator (embodiment #1) and (b) using our custom circulator (embodiment #2). TFP, thin-film polarizer; p-pol, p-polarized beam; s-pol, s-polarized beam; L1, f = 200 mm lens; L2, f = 15.8 mm lens; L3, f = 11.31 mm lens.

4. Results and discussion

We first characterized the performance of the sFPI by spectrally analyzing an attenuated beam from the cw single-frequency fiber-laser. Since the fiber-laser has a linewidth much less than Δf_{FPI}, the resulting spectrum represents the sFPI instrument response. The FPI scan slightly exceeding one FSR is shown in Fig. 3. Given an FSR = 1 GHz (d = 75 mm), we find the FWHM of a resonance peak corresponding to a measured interferometer resolution Δf_{FPI} ~1.5 MHz, as shown in Fig. 3 (inset). We also measured the overall transmission efficiency of the sFPI (in resonance) and found it to be around T_{FPI} = –7.4 dB at 1575 nm.

#193983 - $15.00 USD Received 16 Jul 2013; revised 14 Aug 2013; accepted 22 Aug 2013; published 3 Sep 2013

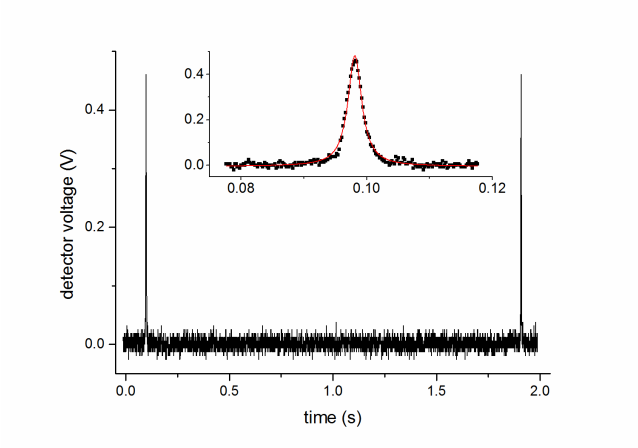

Fig. 3. sFPI output detector voltage V_{det} for a linear ramp voltage V_{ramp} scanning slightly more than a full FSR. One full FSR = 1 GHz corresponds to a measured time interval of 1.81 s. Using the measurement data points comprising the first resonance peak, a Lorentzian fit (red curve of inset) results in a full-width-at-half-maximum of 2.67 ms. This gives a measured sFPI bandwidth Δf_{FPI} = 1.5 MHz.

We also noted that in typical laboratory experiments, the sFPI resonance center frequency can drift unpredictably in the order of ~1 MHz every second primarily due to thermal effects. The rate of frequency drift is too small to affect the measurement of instrument bandwidth in Fig. 3. Nonetheless, this drift is expected to cause a problem for extended velocimetry measurement period (e.g. few minutes or longer) during which the reference resonance peak can drift well outside the scanned frequency range. In future improvement of the setup, we can largely reduce this drift by applying one or a combination of known passive and active means. Passive solutions include improved thermal isolation of the sFPI housing and the use of material with lower thermal expansion coefficient α for the mechanical structure of the interferometer. For example, more than an order of magnitude in thermal stability is expectedly gained from using Invar ($\alpha = 1.2 \times 10^{-6}$/°C at 20 °C) instead of the aluminum ($\alpha = 23.1 \times 10^{-6}$/°C at 20 °C) employed in our current sFPI. Active means may involve automated tuning of either the laser frequency or the V_{offset} to counteract the thermally induced drift.

In the LDV system described in this work, the power levels of both reference and signal beam are sufficiently low – i.e. the measurement sensitivity is limited by the detector electronic noise rather than by optical shot noise. By defining the total optical signal power collected by the LDV receiver as P_s, we can describe the performance of the sFPI-LDV in terms of the minimum detectable P_s corresponding to a signal-to-noise ratio (SNR) of unity:

$$P_s^{\min} = \frac{\mathrm{NEP}\sqrt{\mathrm{B}}}{T_{\mathrm{rec}} T_{\mathrm{FPI}}}, \tag{4}$$

where the product $T_{\mathrm{rec}} T_{\mathrm{FPI}}$ describes the total attenuation factor along the signal path from receiver, through the sFPI and to the detector (Fig. 2). Larger reference beam power means larger optical shot noise contribution (since the finite finesse means complete suppression of the reference beam off resonance is not achievable) which translates to poorer signal sensitivity than what is calculated from Eq. (4). Using Eq. (4) with $T_{\mathrm{rec}} T_{\mathrm{FPI}}$ » –10 dB, we estimate $P_s^{\min}$ to be 0.3 pW. This predicted performance is experimentally confirmed by the results shown in Fig. 4. For the result plotted in Fig. 4, the setup in Fig. 3(b) with 1575 nm fiber-laser as source was used. A more realistic value of signal power easily seen above the noise floor of the detection system is ~10 dB above $P_s^{\min}$. With a detector conversion gain of 0.1 V/pW, the individual incident power onto the detector is found to be 1.2 pW and 0.3 pW

#193983 - $15.00 USD Received 16 Jul 2013; revised 14 Aug 2013; accepted 22 Aug 2013; published 3 Sep 2013

corresponding to reference and signal, respectively. Considering the attenuation along the signal path, the received signal power estimated from Fig. 4 is 2 pW. Thus, using only few off-the-shelf components, we have realized an ultrasensitive instrument for frequency-resolved or velocity-resolved motion sensing of poorly reflecting targets. The associated video clip (Media 1) of Fig. 4 shows a successive series of 100-ms V_{det} plots, i.e. an update rate 10 Hz, depicting the signal peak sufficiently distinguishable from the noise floor fluctuations as predicted. The same video clip shows an average of ten successive 100-ms plots – i.e. updates every second with the x-axis converted to frequency in MHz and the position of the reference peak used as zero frequency. This 1-Hz update rate plot clearly demonstrates the signal with Doppler shift centered around 12 MHz measured at sub-MHz stability.

The measurement update rate of our sFPI-LDV system can be significantly improved since the sFPI time resolution can be in the order of sub-microseconds [13]. However, to increase the update rate of the system, a photodetector with higher bandwidth B (typically having higher NEP value) is necessary to fully capture the sharp resonance peaks without suffering from low-pass filtering effects. Higher detector bandwidth increases P_s^{min} due to the increase in both factors in the numerator of Eq. (4). Nevertheless, in some velocimetry applications like wind tunnel tests and physics of exploding surfaces in which high update rates may be required, one could adjust the amount of received signal power such that $P_s > P_s^{min}$ by particle seeding or applying reflective coatings to surfaces under test. In practical sFPI implementations, one can trade off speed resolution for larger T_{FPI} (i.e. larger Δf_{FPI} for smaller P_s^{min}) by using mirrors that give smaller F – a convenient compromise when the anticipated Doppler shift dynamic range spans a full FSR (i.e. high velocity applications).

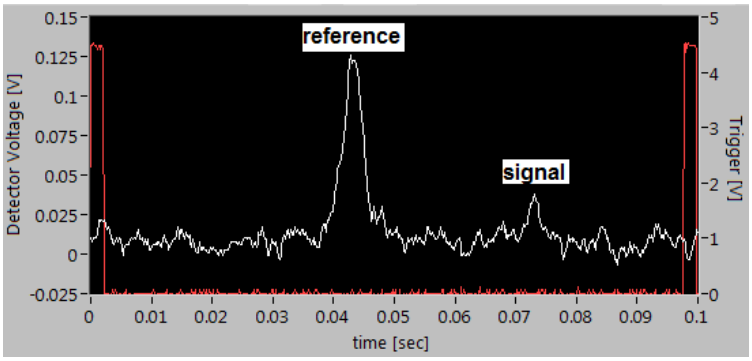

Fig. 4. (Media 1) sFPI detector output voltage versus time for a 100-ms scan period defined by the period of the trigger voltage (same as period of the piezo linear ramp voltage).

The above discussion assumes the measurement is detector or electronic noise limited – that is, optical noise contributions from reference beam and background light (e.g. daylight) are negligible. Background light, already suppressed to a great extent by the sFPI, can be further reduced by inserting additional bandpass optical filter in front of the detector plane. Assuming a reference beam power, P_r, also attenuated along the path from receiver to photodetector characterized by saturation incident power, P_{sat}, the following bound can be suggested:

$$P_r < P_{sat} / (T_{rec} T_{FPI}). \quad (5)$$

For our case where P_{sat} = 100 pW, P_r must not exceed 1 nW. In embodiment #1 shown in Fig. 2(a), this limits the maximum optical power of the laser source to ~1 mW since the reference beam emanates from the inherent leakage from port-1 to port-3 of a standard fiber-optic circulator, in the order of –60 dB. With transmit beam power limited to ~1 mW, the first

#193983 - $15.00 USD Received 16 Jul 2013; revised 14 Aug 2013; accepted 22 Aug 2013; published 3 Sep 2013

sFPI-LDV embodiment is constrained to applications where target backscatter coefficients are relatively high. In embodiment #2 illustrated in Fig. 2(b), a custom circulator design enabled us to significantly reduce the effective leakage to −100 dB. This is achieved due to the fact that free-space optical components of the circulator system can be slightly tilted to prevent unwanted reflections from getting coupled into the interferometer, thus ~1 W (up to 10 W) of laser power can be applied so targets with very low backscatter coefficients can be probed.

5. Conclusion and outlook

We have demonstrated a novel sFPI-based laser Doppler velocimeter implementing a monostatic coaxial architecture. The system operates at 1.5 μm wavelength where eye safety requirement is significantly relaxed and also takes advantage of the high quality, inexpensive and easy-to-access optics and detectors matured within the telecom industry. The predicted high sensitivity down to pW level has been experimentally verified and suggests the potential for atmospheric measurements (and other targets characterized by relatively low backscatter coefficients). We have shown that the increased sensitivity to unwanted backreflections in a coaxial arrangement can be suppressed by several orders of magnitude using a simple custom circulator design. We have also observed that thermal fluctuations affect the sFPI-LDV measurement scheme as a random but slowly varying frequency drift in positions of the resonance peaks. Because our measurement principle enables the simultaneous spectral tracking of signal and reference beams, we have shown that for a hard target at constant speed, the LDV can achieve stable Doppler shift measurement with sub-MHz rms fluctuation.

To improve the system, the frequency drift problem needs to be addressed via improved thermal property of interferometer cavity and/or active control of laser center frequency (e.g. feedback control of laser drive current). Future designs can also consider improvement in the optical transmission efficiency of the interferometer from the current 18% to 50%, which is feasible.

Acknowledgments

The authors would like to acknowledge the Innovation Management of DTU Fotonik for an equipment grant and Finn Pedersen for technical assistance.

#193983 - $15.00 USD Received 16 Jul 2013; revised 14 Aug 2013; accepted 22 Aug 2013; published 3 Sep 2013